Water-Dispersible, Sulfonated Hyperbranched Poly(ether-ketone) Grafted Multiwalled Carbon Nanotubes as Oxygen Reduction Catalysts

Gyung-Joo Sohn,[†] Hyun-Jung Choi,[†] In-Yup Jeon,[†] Dong Wook Chang,[†,‡] Liming Dai,[§] and Jong-Beom Baek*[,†]

[†]Interdisciplinary School of Green Energy/Low-Dimensional Carbon Materials Center, Ulsan National Institute of Science and Technology (UNIST), 100 Banyeon, Ulsan, 689-798, South Korea, [‡]Department of Chemical Systematic Engineering, Catholic University of Daegu, 13-13, Hayang, Gyungbuk, 712-702, South Korea, and [§]Department of Macromolecular Science and Engineering, Case Western Reserve University, 10900 Euclid Avenue, Cleveland, Ohio 44106, United States

ABSTRACT

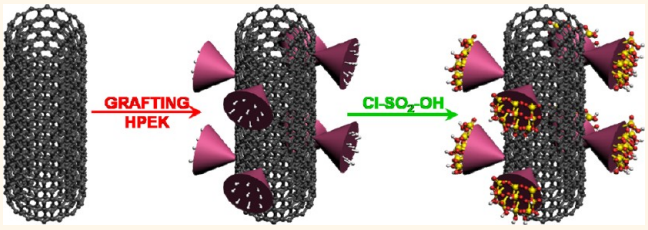

To endorse sufficient water affinity to multiwalled carbon nanotubes (MWCNTs), dendritic hyperbranched poly(ether-ketone) (HPEK) was first covalently grafted to the surface of a MWCNT *via* a Friedel–Crafts acylation reaction. The resultant HPEK-grafted MWCNT (HPEK-g-MWCNT) was subsequently sulfonated in chlorosulfonic acid to produce sulfonated HPEK-g-MWCNT (SHPEK-g-MWCNT), which is dispersible well in water showing a zeta potential value of −57.8 mV. The SHPEK-g-MWCNT paper simply formed by filtration of aqueous dispersion has a sheet resistance as low as 63 Ω/sq. Its thin film shows a high electrocatalytic activity for oxygen reduction reaction (ORR). Thus, the newly produced water-dispersible MWCNT is a new class of high performance cathode material for ORR.

KEYWORDS: water dispersible · multiwalled carbon nanotube · hyperbranched polymer · electrocatalyst · oxygen reduction reaction

During the last few decades, carbon nanotubes (CNTs) have been a focal point for materials research and development due to their excellent physical, electrical and thermal properties.[1−4] For instance, CNTs have been used for polymer-based composites,[5] energy storage materials,[6] electronic devices,[7] biosensors,[8] and many others.[9,10] Although CNTs as nanoscale additives are expected to significantly improve the performances of hybrid materials, there are two critical issues that need to be addressed in order to enhance their properties; that is the homogeneous dispersion with minimal and/or without structural distortion and strong interfacial adhesion between CNTs and supporting matrices. Hitherto, there have been many physical,[11−14] chemical,[15−17] and combined methods[18,19] to optimize stable dispersions of CNTs in foreign matrices. Ultrasonicaiton has been the most favorable physical method for the dispersion of CNTs. It has, however, been known to seriously damage the frameworks of the CNTs by sidewall opening, breaking, and turning the frame into amorphous carbon depending upon dose strength, time, and temperature.[20,21] Thermodynamic gains from enthalpy by bond dissociation and functionalization and entropy by breaking and fragmentation are the primary driving force for the homogeneous dispersion upon sonication after scarifying the high crystallinity and aspect ratio of pristine CNTs. On the other hand, treatment with corrosive and oxidative acids, such as nitric acid, sulfuric acid and their mixture, is the most commonly used chemical method for the functionalization of CNTs.[22−24] Similar to conversion of graphite into graphite oxide/graphene oxide (GO),[25−27] corrosive oxidation has long been exploited. The treatments of corrosive acids turn CNTs into CNT-oxides (Theoretically, curvature CNT should be more reactive than plane graphite due to C−C bond strain and larger surface area). As observed in GO,[28] the electrical insulating and defective nature of CNT-oxides does not display properties outstanding from those of pristine CNTs, leaving the CNT research lagging behind the booming graphene research.[29,30] Even after a homogeneous dispersion is achieved in common organic media to provide processability, the interaction between CNTs and supporting

* Address correspondence to jbbaek@unist.ac.kr.

Received for review April 27, 2012 and accepted June 10, 2012.

Published online June 10, 2012
10.1021/nn301863d

matrices becomes a secondary consideration in the use as reinforcing additives. Thus, considering the critical issues in CNT research, an efficient chemical modification of CNTs without causing CNT damages and their dispersion in eco-friendly media for convenient processing still remain as an important challenge.

Here, we report water-dispersible multiwalled carbon nanotubes (MWCNTs), which were prepared in a simple two-step reaction. Dendritic hyperbranched poly(ether-ketone) (HPEK) was first grafted to the surface of as-received MWCNTs by *in situ* polycondensation of 3,5-diphenoxybenzoic acid as an AB_2 monomer *via* "direct" Friedel–Crafts acylation in a mild polyphosphoric acid (PPA)/phosphorus pentoxide (P_2O_5) medium.[31,32] The reaction medium is known to be nondestructive through the sp^2 hybrid C–H defect-selective functionalization of CNTs.[33] Dendritic macromolecules such as dendrimers and hyperbranched polymers consist of highly branched 3-dimensional (3D) structures with the large number of periphery functional groups,[34] to which can be utilized for further chemical modification. Thus, the resultant HPEK grafted MWCNT (HPEK-g-MWCNT) was able to provide numerous reactive sites for subsequent sulfonation in chlorosulfonic acid. The hydrophilic nature of the sulfonated HPEK-g-MWCNT (SHPEK-g-MWCNT) was expected to display water-dispersibility by introducing oxygenated groups on its periphery without any further damage to CNT framework. In this way, CNTs could have dispersibility (processability) in desired media with their aspect ratio and structural integrity preserved. As a result, CNT-based functional materials are expected to display a maximum enhanced performance for electrocatalytic activity, and they are also useful for eco-friendly spray coating applications.

RESULTS AND DISCUSSION

Taking advantages of the characteristic natures of 3D dendritic macromolecules,[34] water-dispersible multiwalled carbon nanotubes (MWCNTs) were prepared.[35,36] To covalently anchor dendritic macromolecules to the surface of MWCNTs and endorse hydrophilic nature, a two-step reaction sequence involving Friedel–Crafts acylation in a mild polyphosphoric acid (PPA)/phosphorus pentoxide (P_2O_5) medium and subsequent sulfonation in chlorosulfonic acid (Cl–SO_2–OH) was applied. The Friedel–Crafts acylation in a PPA/P_2O_5 medium is known to be nondestructive and defect-selective functionalization for sp^2 hybrid C–H.[33] To estimate the inherent sp^2 hybrid C–H defects on MWCNTs for the reaction, elemental analysis (EA) was conducted (Table S1, see the Supporting Information). "Pristine" MWCNTs contain a significant amount of hydrogen (0.30 wt%, converting into atomic percent could suggest the number of available sp^2 hybrid C–H per carbons), which is attributable to the inherent sp^2 hybrid C–H defects. The result indicates an upper limit of one hydrogen atom attached for every 28 carbon atoms (see Supporting Information, Table S1). The available sp^2 hybrid C–H defects on the MWCNT are anchoring sites for dendritic macromolecules in PPA/P_2O_5 medium as nondestructive functionalization *via* the Friedel–Crafts acylation reaction. The reaction medium, PPA with an optimized amount of P_2O_5, is benign and does not damage the MWCNT but is strong enough to selectively functionalize at the sp^2 hybrid C–H defects.[33] PPA is a viscous polymeric acid, which can provide strong shear to promote efficient dispersion of CNTs during mechanical stirring and to impede reaggregation after dispersion. In addition, it has a mild acidity (pk_a = ~2.1), which is about the same as gastric acid (pk_a = 1.3–3.5), so it does not oxidize and damage the CNT framework.[31–33] Thus, PPA has many advantages for functionalization of carbon-based nanomaterials over the commonly used corrosive acids such as nitric acid (pk_a = −1.5)/sulfuric acid (pk_a = −3.0) mixture for the synthesis of CNT-oxides.[37] The role of P_2O_5 is the removal of a water molecule, which is generated as a byproduct from the dehydration of carboxylic acid during the course of Friedel–Crafts reaction. As described in Supporting Information,

Figure S1 in ESI, the reaction between P_2O_5 and water results in increasing molecular weight of PPA, suppressing backward reaction and promoting forward reaction. To covalently graft hyperbranched poly(ether-ketone) (HPEK) to the surface of MWCNTs, the AB_2 monomer, 3,5-diphenoxybenzoic acid, was synthesized by following the literature report (see detailed preparation and characterization in the Experimental section and Supporting Information, Figure S2 in ESI).[38] A pristine MWCNT was grafted with HPEK by *in situ* polymerization of the monomer in a PPA/P_2O_5 medium to produce HPEK-g-MWCNT (Figure 1a, chemical structures of monomer and HPEK-g-MWCNT delineated in the Supporting Information, Figure S3). The viscosity of the reaction mixture was increased as grafting of HPEK to the surface of the MWCNT proceeded (Figure 1b). Interestingly, the photograph of the reaction mixture showed dark-green color with flash light (Figure 1c), indicating that HPEK was uniformly grafted to the surface of MWCNT and the resultant HPEK-g-MWCNT was homogeneously dispersed in the reaction medium. The dark powder that precipitated upon pouring into distilled water was collected by suction filtration and washed with water. To minimize unexpected variables, the product was completely worked up by Soxhlet extraction with water and methanol to remove the reaction medium and low molar mass impurities, respectively. It was further washed with dichloromethane, which is a good solvent for HPEK,[38] to get rid of free HPEK and dried to give 60.3% yield. Elemental analysis (EA) determined on the basis of yield is in good agreement between theoretical and

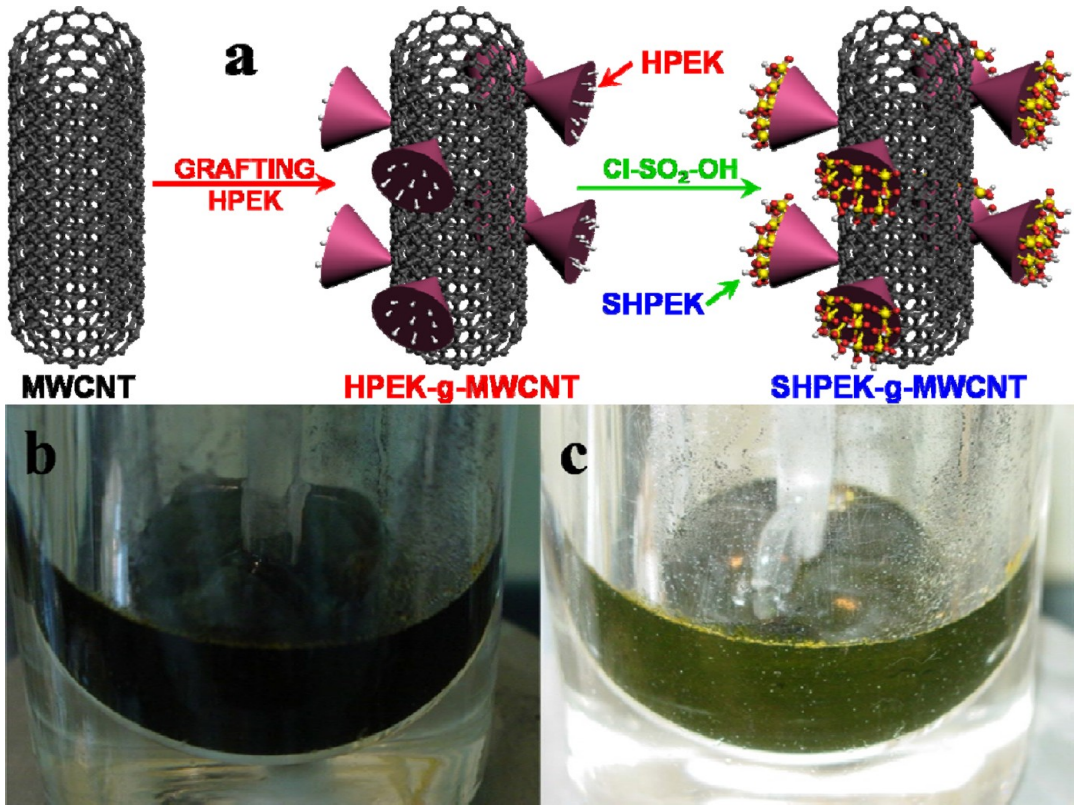

Figure 1. (a) Schematic demonstrations for the covalent grafting of HPEK to the surface of MWCNTs in PPA/P_2O_5 medium and subsequent sulfonation of HPEK-g-MWCNT in chlorosulfonic acid to yield SHPEK-g-MWCNT. Photographs taken from the reaction flask of HPEK-g-MWCNT in PPA/P_2O_5: (b) without and (c) with flash light. Deep green color with flash light indicated a homogeneous dispersion of HPEK-g-MWCNT after uniform grafting of HPEK to the surface of MWCNT.

experimental CHO counts (Supporting Information, Table S1).

The HPEK-g-MWCNT was subsequently sulfonated in chlorosulfonic acid to produce sulfonated HPEK-g-MWCNT (SHPEK-g-MWCNT) (Figure 1a). For comparison, direct sulfonation of pristine MWCNT in chlorosulfonic acid was also carried out in the same sulfonation condition for the synthesis of SHPEK-g-MWCNT. Resultant sulfonated MWCNT (S-MWCNT) (Supporting Information, Figure S4a) has only a sulfonic acid per 855 carbons (C/S = 855, see Supporting Information, Table S1). As a result, the S-MWCNT is not dispersible in water, indicating that direct sulfonation to MWCNT is not enough to introduce a large number of sulfonic acid groups. Thus, to provide enough reactive sites for sulfonation, grafting of dendritic HPEK onto the surface of MWCNT is necessary. The number of available activated sites (sp^2 hybrid C−H) by ether−phenyl are tremendously increased to n(DP + 1),[34] where n is an average number of HPEKs covalently attached to MWCNT, and DP stands for an average degree of polymerization (Supporting Information, Figure S4b). The sulfonation of HPEK-g-MWCNT could introduce a large number of sulfonic acids to the periphery of HPEK-g-MWCNT and makes sulfonated HPEK-g-MWCNT (SHPEK-g-MWCNT) hydrophilic enough to be well dispersed in water.[8] The SHPEK-g-MWCNT has a sulfonic acid per 85 carbons (see Supporting Information, Table S1). The degree of sulfonation in SHPEK-g-MWCNT could be increased almost 10 times as high as that of S-MWCNT.

Due to dissociation of the sulfonic acids in water *ca.* 100% and to become negatively charged,[39] the SHPEK-g-MWCNT is indeed well dispersible in polar aprotic solvents such as *N,N*-dimethylacetamide (DMAc) and *N*-methyl-2-pyrrolidone (NMP). It is also well dispersible in polar protic solvents such as methanol, ethanol, and water (Supporting Information, Figure S5). Zeta potential indicates the degree of repulsion between adjacent, similarly charged particles in dispersion. For molecules and particles that are small enough, a high zeta potential value will confer stability; that is, the solution or dispersion will resist aggregation. When the potential is low, attraction exceeds repulsion and the dispersion will break and flocculate. The aqueous dispersion of SHPEK-g-MWCNT (17.4 mg in 500 mL water) shows −57.8 mV (Figure 2a). This value is considered to be a "good stability" of colloidal dispersion (Supporting Information, Table S2) and among the highest absolute values even reported for carbon-based nanomaterials.[39,40]

To ensure the covalent attachment of HPEK to the HPEK-g-MWCNT and sulfonic acids on SHPEK-g-MWCNT, samples were subjected to FT-IR analysis. Spectra from

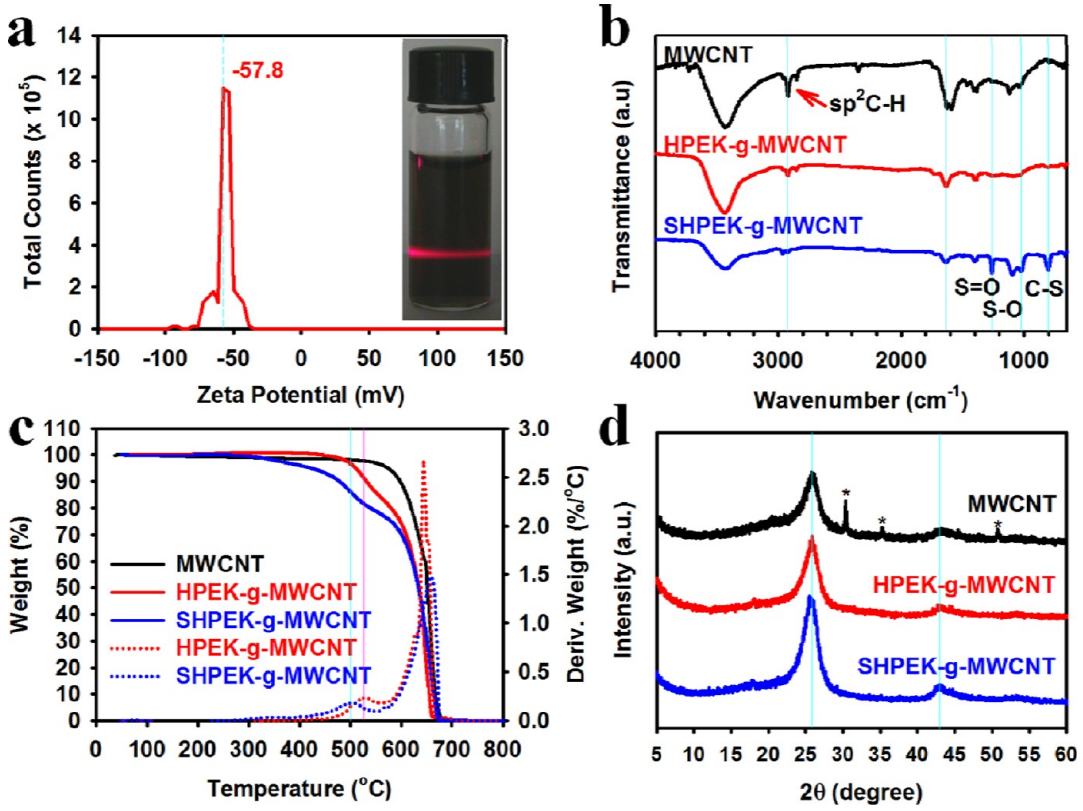

Figure 2. (a) Zeta-potential curve of SHPEK-g-MWCNT (17.4 mg) solution in water (500 mL). Inset is a photograph of the solution with hand-held laser shining; (b) FT-IR spectra (KBr pellets); (c) TGA thermograms obtained with ramping rate of 10 °C/min in air; (d) XRD powder patterns of samples.

HPEK-g-MWCNT and SHPEK-g-MWCNT exhibit absorption peaks at 2918 and 2842 cm^{-1} corresponding to sp^2 hybrid C−H and sp^3 hybrid C−H stretching bands, respectively. They also show aromatic carbonyl (C═O) and C═C peaks at 1640 and 1383 cm^{-1}, respectively (Figure 2b). The strong hydroxyl stretching vibrations appearing at 3435 cm^{-1} is moisture present in KBr. SHPEK-g-MWCNT shows characteristic S═O and S−O stretching bands at 1263 and 1100−1027 cm^{-1}, respectively, and a peak at 805 cm^{-1} is assignable to C−S vibration. The result is clear evidence for sulfonic acids on SHPEK-g-MWCNT.

The degree of HPEK grafting and subsequent sulfonation could be quantitatively estimated by thermogravimetric analysis (TGA) in air. HPEK-g-MWCNT and SHPEK-g-MWCNT show stepwise weight loss, while pristine MWCNTs are stable to 600 °C (Figure 2c). In the case of HPEK-g-MWCNT, the weight loss occurring in the temperature range from 500 to 600 °C is related to HPEK covalently attached to the surface of MWCNTs. The amount of HPEK grafts is approximately 25 wt %. In the case of SHPEK-g-MWCNT, two-step weight loss was observed. The initial weight loss started from 330 to 500 °C, which could be attributable to the decomposition of sulfonic acids in the form of SO_3,[41] was approximately 10 wt %. The second step weight loss from 500 to 600 °C should be originated from the decomposition of HPEK moiety, which was thermo-oxidatively stripped off from MWCNT surface in air.[38] In all cases, char yields at 800 °C approached zero, indicating that there were almost no persisting metallic impurities that presented in MWCNT (*vide infra*).

The role of the reaction medium, PPA/P_2O_5, was also studied by wide-angle X-ray diffraction (WAXD). If the reaction condition and workup procedures could damage MWCNT framework, its crystallinity should be diminished. However, the peak intensities at 25.54°, which is related to wall-to-wall distance of MWCNT, were increased as reaction steps increased (Figure 2d). The result suggests that HPEK grafting in PPA/P_2O_5 and sulfonation in chlorosulfonic acid are purifying rather than damaging MWCNT.[33,37] Residual metallic impurities (denoted by the asterisk (∗)) had completely disappeared from pristine MWCNT. The HPEK-g-MWCNT does not show peaks from residual catalysts but displays a strong interlayer *d*-spacing value at 3.48 Å (2θ = 25.54°). Similarly, SHPEK-g-MWCNT displayed a more prominent interlayer *d*-spacing value at 3.44 Å (2θ = 25.9°).

The X-ray photoelectron spectroscopy (XPS) survey of pristine MWCNTs shows a strong C 1s peak at 284.5 eV and a very weak O 1s at 533.0 eV (Figure 3a), which is mainly attributable to physically adsorbed oxygen to the surface of graphitic carbon.[42] The HPEK-g-MWCNT also displays a strong C 1s peak at 284.5 eV and relatively stronger O 1s peak due to the

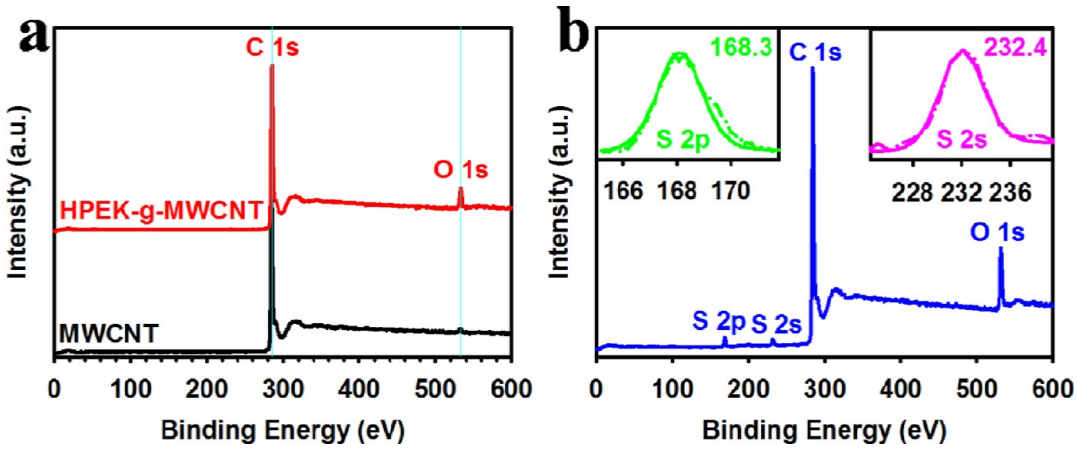

Figure 3. XPS spectra: (a) MWCNT and HPEK-g-MWCNT; (b) SHPEK-g-MWCNT. Insets are S 2p (left) and S 2s (right) peaks.

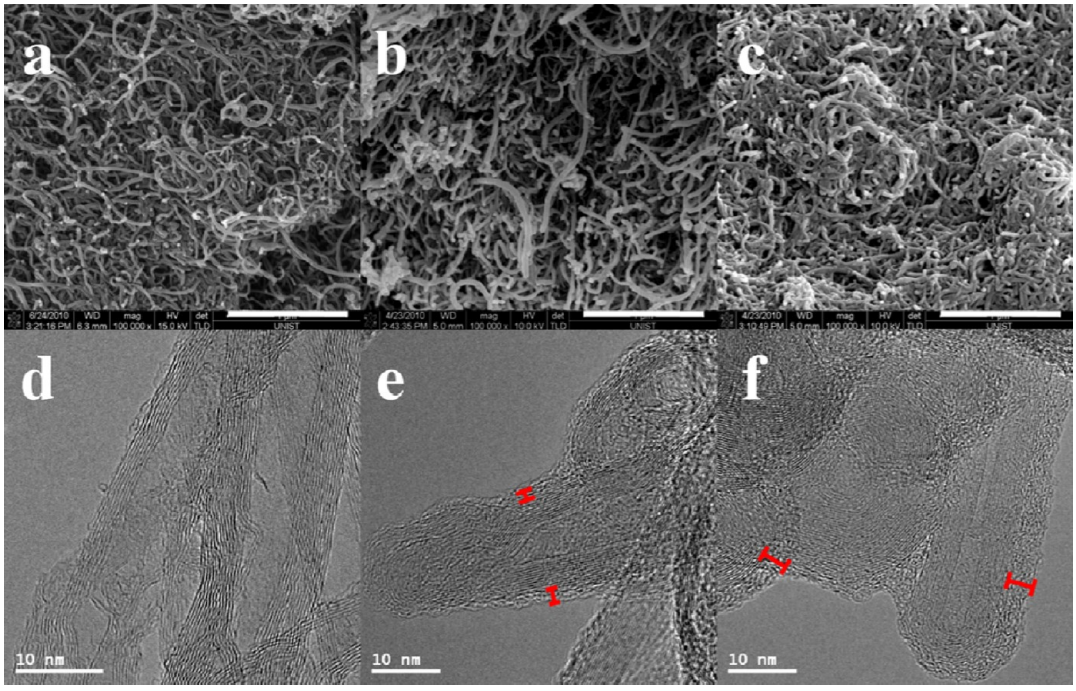

Figure 4. SEM images: (a) pristine MWCNT; (b) HPEK-g-MWCNT; (c) SHPEK-g-MWCNT. Scale bars are 1 μm. TEM images: (d) pristine MWCNT; (e) HPEK-g-MWCNT; (f) SHPEK-g-MWCNT.

contribution from carbonyl (C═O) and ether (-O−) in HPEK (Figure 3a). In the case of SHPEK-g-MWCNT, XPS survey displays typical C 1s and O 1s peaks at 284.5 and 533.0 eV, respectively (Figure 3b). Because of the the sulfonic acids on its periphery, SHPEK-g-MWCNT shows characteristic S 2p and S 2s peaks at 168.3 and 232.4 eV, respectively (Figure 3b, insets).[43] The S 2p peak is assignable to S $2p_{3/2}$ electron, confirming an efficient sulfonation of HPEK to convert SHPEK.

SEM images were obtained from pristine MWCNT, HPEK-g-MWCNT, and SHPEK-g-MWCNT. Pristine MWCNT has tube diameter and length in the range of 10−20 nm and 10−50 μm, respectively, showing spaghetti-like network with smooth and clean surface (Figure 4a). Due to the HPEK and SHPEK coated on the MWCNT, overall tube diameter dimensions of HPEK-g-MWCNT and SHPEK-g-MWCNT are increased to 30−40 nm, while their tube lengths remain almost constant (Figure 4b, 4c and Supporting Information, Figure S6). Furthermore, there are no free HPEK and SHPEK observed, implying that free polymers were completely washed off during workup procedures (multiple Soxhlet extraction). In conjunction with TGA, the results strongly support that HPEK has been uniformly grafted onto the surface of MWCNT, and HPEK has also been efficiently sulfonated to be SHPEK. Furthermore, SEM element mapping clearly displays the uniform distribution of C, O, and S elements (Supporting Information, Figure S7a−d). Energy dispersive X-ray spectroscopy (EDX) confirms

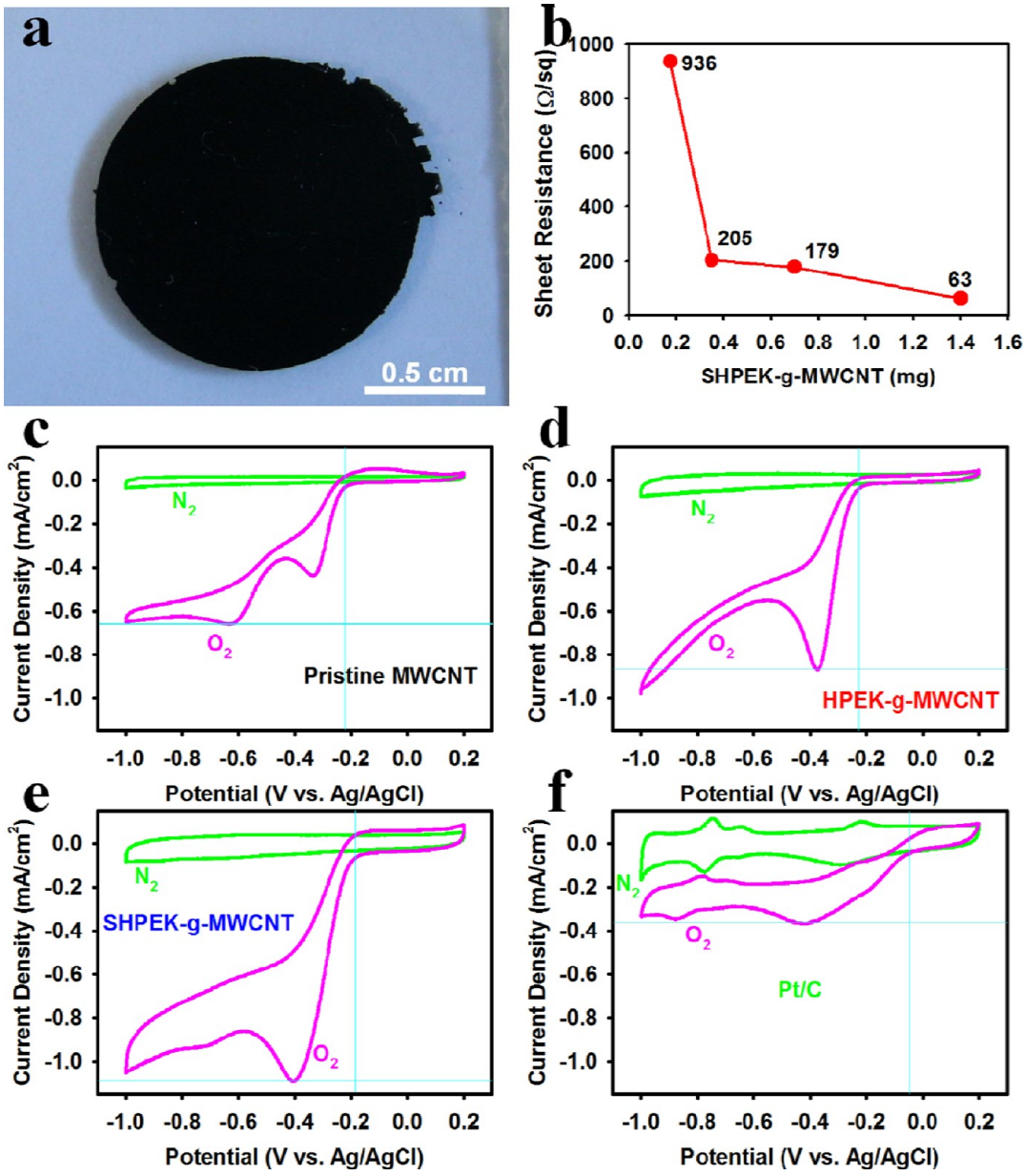

Figure 5. (a) Photograph of freestanding SHPEK-g-MWCNT paper (1.5 cm) prepared from filtration of SHPEK-g-MWCNT dispersed solution in water; (b) sheet resistance changes as a function of SHPEK-g-MWCNT weight at given diameter (1.5 cm). Cyclic voltammograms of sample films on glassy carbon (GC) electrodes in nitrogen- and oxygen-saturated 0.1 M aqueous KOH solution with a scan rate of 10 mV/s; (c) pristine MWCNT; (d) HPEK-g-MWCNT; (e) SHPEK-g-MWCNT; (f) Pt/C.

the S concentration on the surface of MWCNT (Figure S7e). The weight percent of S was detected as high as 4.7 wt % (Figure S7e), a value that is more than twice that from the EA result (2.07%, Table S1). The discrepancy may be originated from the sensitivity difference between two methods. EDX is known to be more regionally sensitive to the chemical composition than EA,[44] whose result would be more reliable for quantitative estimation of element contents in a bulk state. HPEK-g-MWCNT consists of C, H, and O, while SHPEK-g-MWCNT is composed of C, H, O, and S. The sole presence of S in SHPEK-g-MWNCT indicates that a significant number of sulfonic acids have been introduced to the surface of the SHPEK-g-MWCNT (see Supporting Information, Table S1).

To further visually ensure the uniform grafting and subsequent sulfonation, the dispersed solutions of pristine MWCNT, HPEK-g-MWCNT and SHPEK-g-MWCNT in ethanol were very much diluted. The solutions were dropped to the carbon coated grid and vacuum-dried. As shown in Figure 4d, the surface of pristine MWCNT is clean and smooth with clear stripes originated from its high crystalline graphitic walls. In the case of HPEK-g-MWCNT, inner core MWCNT with stripes is uniformly decorated by HPEK with outer layer thickness of ~2 nm (Figure 4e). Similarly, the outer layer of

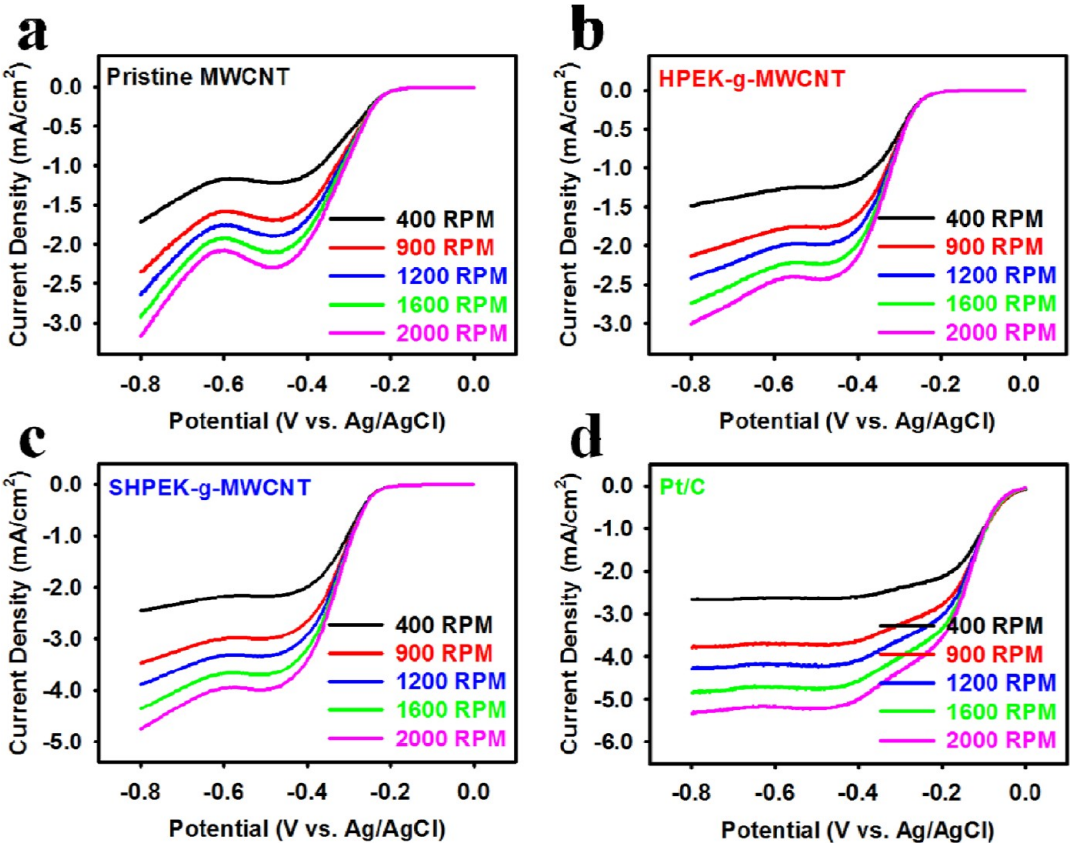

Figure 6. RDE voltammograms in oxygen-saturated 0.1 M aq KOH solution with a scan rate of 0.01 V/s at different rotating rates of 400, 900, 1200, 1600, and 2000 rpm: (a) pristine MWCNT; (b) HPEK-g-MWCNT; (c) SHPEK-g-MWCNT; (d) Pt/C.

SHPEK-g-MWCNT is coated by SHPEK with thickness of ~4 nm. The increase in thickness of SHPEK layer compared to HPEK is due possibly to intramolecular charge repulsion between sulfonic acids. The stripes of inner cores implicate that MWCNTs of HPEK-g-MWCNT and SHPEK-g-MWCNT remain structurally intact during reactions and workup procedures, again, implying that both grafting and sulfonation applied in this work do not structurally damage.

Having structural confirmation and solubility information, freestanding SHPEK-g-MWCNT papers were also prepared by a simple filtration of the dispersed solution in water through an alumina membrane (pore size = 0.2 μm) (Figure 5a). Depending on the amounts of SHPEK-g-MWCNT at a given diameter (1.5 cm), sheet resistance was reduced to as low as 63 Ω/sq (Figure 5b). The low sheet resistance should originate from maintaining tube length and providing a low percolation threshold of SHPEK-g-MWCNT (Figure 4c), which has a high aspect ratio even after grafting and sulfonation. To our best knowledge, this work is the first demonstration of a freestanding MWCNT paper prepared from a water dispersible MWCNTs without destructive chemical oxidation.[45]

In addition to low sheet resistance (high electrical conductivity), which is a prerequisite for a high performance electrode, a large number of sulfonic acids on its periphery make SHPEK-g-MWCNT hydrophilic to efficiently absorb oxygen.[46] SHPEK-g-MWCNT is thus expected to display a good electrocatalytic activity for oxygen reduction reaction (ORR). Hence, the SHPEK-g-MWCNT (0.5 mg) solution in DMAc (1.5 mL) was drop-coated on a glassy carbon (GC) electrode. For comparison, pristine MWCNT, HPEK-g-MWCNT, and platinum (Pt) on activated carbon (Pt/C, Vulcan XC-72R) electrodes were also prepared at the same condition. Although featureless voltammetric currents from three metal-free electrodes (pristine MWCNT, HPEK-g-MWCNT, and SHPEK-g-MWCNT) were observed in N_2 saturated 0.1 M aqueous KOH solution within the potential range of −1.0−0.2 V, the SHPEK-g-MWCNT showed higher capacitance than MWCNT and HPEK-g-MWCNT (Figure 5c−e and Supporting Information, Table S3). In O_2 saturated solution, on the other hand, pristine MWCNT, HPEK-g-MWCNT and SHPEK-g-MWCNT electrodes displayed a dramatic increase in voltametric current by more than 2.7, 1.9, and 2.8 times (Figure 5d,e), respectively, compared to the current observed in N_2 saturated electrolyte. The results indicated that the pristine MWCNT, HPEK-g-MWCNT, and SHPEK-g-MWCNT all have high electrocatalytic activity for ORR. Among them, SHPEK-g-MWCNT is much more efficient than the pristine MWCNT and HPEK-g-MWCNT in terms of low overpotential, high current density and capacitance

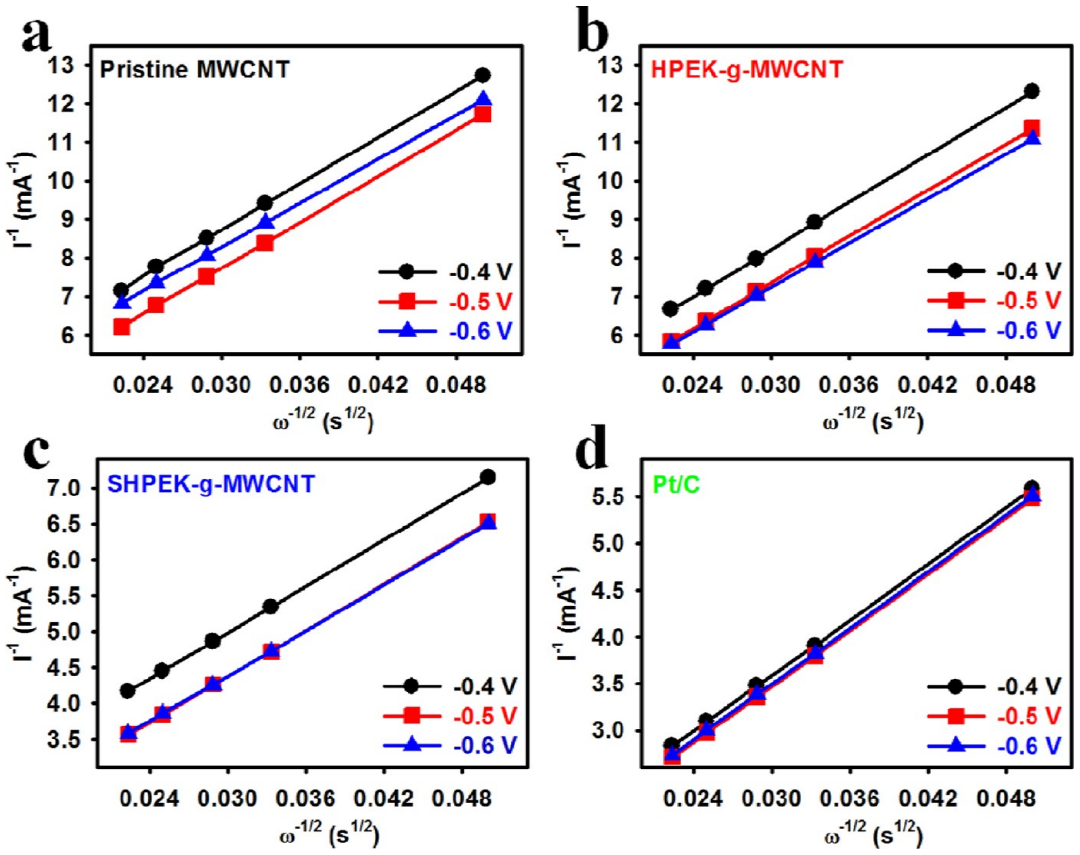

Figure 7. (a) Koutecky−Levich plots derived from RDE measurements at different electrode potentials (black line, −0.4 V; red line, −0.5 V; and blue line, −0.6 V): (a) pristine MWCNT; (b) HPEK-g-MWCNT; (c) SHPEK-g-MWCNT; (d) Pt/C. On the basis of RDE results of samples, the transferred electron number per oxygen molecule involved in the oxygen reduction is calculated.

(Supporting Information, Table S3). More importantly, the maximum current density of SHPEK-g-MWCNT is −1.10 mA/cm^2 at −0.41 V, which is approximately three times higher than that (−0.37 mA/cm^2 at −0.42 V) of commercial Pt/C. Last but not least, the capacitance of SHPEK-g-MWCNT (151 F/g) is 1.8 times higher than that of commercial Pt/C (85 F/g) in oxygen-saturated 0.1 M KOH solution (Supporting Information, Table S3). The origin of superb ORR activity of SHPEK-g-MWCNT in base condition should be due to its much higher hydrophilic nature and stronger polyelectrolyte effect. The ionic interaction between sulfonic acids on SHPEK-g-MWCNT and KOH in electrolyte makes SHPEK-g-MWCNT hydrophilic, and thus it has better affinity to aqueous medium as well as oxygen. Furthermore, SHPEK grafts on MWCNT should be a fully extended conformation by negative charge repulsions, allowing efficient oxygen diffusion to the MWCNT for better ORR performance. Furthermore, HPEK-g-MWCNT displayed good cycle stability maintaining 97% of initial capacitance after stabilization (10 cycles) for 24000 s, while Pt/C showed only 86% (Supporting Information, Figure S8). Thus, we believe SHPEK-g-MWCNT could be promising electrocatalyst for ORR.

To gain further insight into the role of sample electrodes during the ORR process, the reaction kinetics by rotating-disk electrode (RDE) was investigated (Figure 6). The oxygen reduction activity of the SHPEK-g-MWCNT (Figure 6c) is obviously more pronounced than pristine MWCNT (Figure 6a) and HPEK-g-MWCNT (Figure 6b) and similar to that of commercial Pt/C (Figure 6d). In all cases, the voltammetric profiles showed that the current density was increased by increasing rotating rate. The onset potentials of pristine MWCNT, HPEK-g-MWCNT, and SHPEK-g-MWCNT for ORR were similar around −0.22 V (Figure 6a−c). In all cases, the corresponding Koutecky−Levich plots at electrode potential ranges of −0.4 to *ca.* −0.6 V revealed first-order reaction kinetics with respect to the concentration of dissolved O_2 (Figure 7).[47] As described the detailed kinetic analysis in the Experimental section, the number of transferred electrons (*n*) involved in the oxygen reduction can be analyzed on the basis of the Koutecky−Levich equation.[48] The *n* was calculated to be approximately 2.0 for both pristine MWCNT and HPEK-g-MWCNT (Figure 7 and Supporting Information, Table S4), indicating they have a two-electron transfer in an oxygen reduction process. However, the *n* value obtained from SHPEK-g-MWCNT was approximately 3.7, suggesting that the SHPEK-g-MWCNT led to a four-electron process, which is similar to commercial Pt/C.

CONCLUSIONS

Multiwalled carbon nanotubes (MWCNTs) have inherent sp^2 hybrid C−H defects for the electrophilic substitution reaction. To introduce abundant reactive sites to the surface of a MWCNT without further oxidative damages, dendritic hyperbranched poly(ether-ketone) (HPEK) was grafted onto the surface of the MWCNT to produce HPEK-grafted MWCNT (HPEK-g-MWCNT). The HPEK-g-MWCNT could provide numerous active sites for subsequent sulfonation to afford sulfonated HPEK-g-MWCNT (SHPEK-g-MWCNT). The covalent grafting and sulfonation of MWCNT were confirmed with various analytical techniques. The resultant SHPEK-g-MWCNT was well dispersible in water with a zeta potential of −57.8 mV (good stability). Freestanding SHPEK-g-MWCNT paper displays sheet resistance as low as 63 Ω/sq and high electrocatalytic activity for oxygen reduction reaction (ORR) without heteroatom doping onto the MWCNT framework. Hence, the approach is a unique wet-chemical functionalization route that does not require initial oxidative damage to the MWCNT framework. Water-dispersible SHPEK-g-MWCNT can be eco-friendly processed by a simple (spray) coating for uses in various applications such as biological technologies, fuel cells (this work),[46] batteries,[49] sensors, and opto-electronics in practice.

EXPERIMENTAL SECTION

Materials. All reagents and solvents were purchased from Aldrich Chemicals Inc. and used as received. Multiwalled carbon nanotubes (CVD MWCNT 95 with diameter of ~20 nm and length of 10−50 μm) were obtained from Hanwha Nanotech, Incheon, South Korea.

Instrumentations. Fourier-transform infrared (FT-IR) spectra data were recorded on a Jasco Fourier transform spectrophotometer model 480 Plus. All samples were mixed with KBr powder and pressed to make semitransparent pellets. The data were collected in the wavelength range from 650 to 4000 cm^{-1}. Elemental analyses (EA) were performed with a CE Instruments EA1110. Thermogravimetric analysis (TGA) was conducted in air atmospheres with a heating rate of 10 °C/min using a TA Q200. X-ray photoelectron spectroscopy (XPS) analysis was carried out on a Thermo Fisher K-alpha instrument employing monochromatic A1 Kα radiation as the X-ray source. Powder X-ray diffraction (XRD) measurements were carried out using a Rigaku DMax/2000PC with a Cu target tube. The field emission scanning electron microscopy (FE-SEM) used in this work was FEI NanoSem 230. The high resolution transmission electron microscope (HR-TEM) employed in this work was a JEOL JEM-2100F (Cs) operating at 200 kV. The TEM samples were prepared by dropping a solution of dispersed samples in water. Zeta potential measurements were performed with Malvern Nano ZS.

***In-situ* Grafting of HPEK onto MWCNT.** Into a resin flask equipped with a high torque mechanical stirrer, nitrogen inlet and outlet, 3,5-diphenoxybenzoic acid (2.0 g, 6.53 mmol), MWCNTs (2.0 g), polyphosphoric acid (PPA, 80.0 g, 83% P_2O_5 assay), and phosphorus pentoxide (P_2O_5, 20.0 g) were placed. The reaction flask was immersed in an oil bath, and the reaction mixture was stirred under dry nitrogen purge. The flask was heated to 100 °C for 1 h and further heated to 130 °C and maintained for 72 h. The homogeneous reaction mixture was poured into distilled water and the precipitates were collected by suction filtration. The dark black solids were transferred to extraction thimble and Soxhlet-extracted with water for 3 days to completely remove residual reaction medium and with methanol for 3 more days to get rid of low-molar-mass HPEK and other possible organic impurities. The sample was finally freeze-dried at −80 °C under reduced pressure (0.01 mmHg) for 48 h to give 3.21 g of black powders. Free-standing high-molar-mass HPEK was further washed off by Soxhlet extraction with dichloromethane. The final product (HPEK-g-MWCNT) was freeze-dried to give 2.34 g (60.3% yield) of black powder. Anal. Calcd for $C_{157.76}H_{13}O_3$ (calculated on the basis of yield): C, 96.91%; H, 0.66%; O, 2.42%. Found: C, 94.95%; H, 0.65%, O, 4.39%.

Sulfonation of HPEK-g-MWCNT in Chlorosulfonic Acid. Into the one-necked round-bottom flask equipped with a magnetic stirrer, nitrogen inlet, and a dropping funnel, 0.5 g of HPEK-g-MWCNTs was placed. Chlorosulfonic acid (99%, 50 mL) was slowly added, and the mixture stirred at room temperature for 4 h. The reaction flask was immersed in an ice bath, and distilled water was slowly added for 1 h. The precipitates, which settled at the bottom of the flask, were collected by filtration and washed with 1 M aq HCl solution (50 mL) 10 times. The final product was freeze-dried at −80 °C under reduced pressure (0.01 mmHg) for 48 h to give to give 0.55 g of dark powder. Anal. Calcd for $C_{125.99}H_{14}O_6S_1$ (calculated on the basis of yield): C, 91.41%; H, 0.85%; O, 5.80%; S, 1.94%. Found: C, 86.21%; H, 0.76%; O, 9.03%; S, 2.07%.

Electrochemical Study. Cyclic voltammetry (CV) measurements were performed using a computer-controlled potentiostat (CHI 760 C, CH Instrument) in a standard three-electrode cell. A samples/glassy carbon (GC) electrode was used as the working electrode, a platinum wire was the counter electrode, and an Ag/AgCl (3 M KCl filled) electrode was the reference electrode. Rotating disk electrode (RDE) experiments were carried out on a MSRX electrode rotator (Pine Instrument) and the CHI 760 C potentiostat. For all CV and RDE measurements, an aqueous solution of KOH (0.1 M) was used as the electrolyte. N_2 or O_2 was used to purge the solution to achieve oxygen-free or oxygen-saturated electrolyte solution.

The procedure of GC electrode pretreatment and modification are described as follows: prior to use, the working electrode was polished with alumina slurry to obtain a mirror-like surface and then washed with DI water and allowed to dry. Samples (1 mg) were dissolved in 1 mL of solvent mixture of Nafion (5%) and EtOH/water (v/v = 1:9) by sonication. The sample suspensions (5 μL) were pipetted on the glassy carbon (GC) electrode surface, followed by drying at room temperature. The detailed kinetic analysis was conducted according to Koutecky−Levich plots:

$$\frac{1}{j} = \frac{1}{j_k} + \frac{1}{B\omega^{0.5}} \quad (1)$$

where j_k is the kinetic current and B is Levich slope which is given by

$$B = 0.2nF(D_{O_2})^{2/3}\nu^{-1/6}C_{O_2} \quad (2)$$

Here n is the number of electrons transferred in the reduction of one O_2 molecule, F is the Faraday constant (F = 96485 C/mol), D_{O_2} is the diffusion coefficient of O_2 (D_{O_2} =1.9 × 10^{-5} cm^2 s^{-1}), ν is the kinematics viscosity for KOH (ν = 0.01 cm^2 s^{-1}) and C_{O_2} is the concentration of O_2 in the solution (C_{O_2} = 1.2 × 10^{-6} mol cm^{-3}). The constant 0.2 is adopted when the rotation speed is expressed in rpm.

Conflict of Interest: The authors declare no competing financial interest.

Acknowledgment. This research was supported by WCU (World Class University), US-Korea NBIT and Basic Research Laboratory (BRL) programs through the National Research Foundation (NRF) of Korea funded by the Ministry of Education, Science and Technology (MEST), and US Air Force Office of

Scientific Research through Asian Office of Aerospace R&D (AFOSR-AOARD).

Supporting Information Available: Chemical structures, photograph, SEM images, EDX, EA, zeta potential, chronoamperometry, and kinetic data. This material is available free of charge *via* the Internet at http://pubs.acs.org.

REFERENCES AND NOTES

1. Ebbesen, T. W.; Lezec, H. J.; Hiura, H.; Bennett, J. W.; Ghaemi, H. F.; Thio, T. Electrical Conductivity of Individual Carbon Nanotubes. *Nature* **1996**, *382*, 54–56.
2. Iijima, S. Helical Microtubules of Graphitic Carbon. *Nature* **1991**, *354*, 56–58.
3. Jin, Z.; Pramoda, K. P.; Xu, G.; Goh, S. H. Dynamic Mechanical Behavior of Melt-Processed Multiwalled Carbon Nanotube/Poly(Methyl Methacrylate) Composites. *Chem. Phys. Lett.* **2001**, *337*, 43–47.
4. Treacy, M. M. J.; Ebbesen, T. W.; Gibson, J. M. Exceptionally High Young's Modulus Observed for Individual Carbon Nanotubes. *Nature* **1996**, *381*, 678–680.
5. Moniruzzaman, M.; Winey, K. I. Polymer Nanocomposites Containing Carbon Nanotubes. *Macromolecules* **2006**, *39*, 5194–5205.
6. Frackowiak, E.; Béguin, F. Carbon Materials for the Electrochemical Storage of Energy in Capacitors. *Carbon* **2001**, *39*, 937–950.
7. Anantram, M. P.; Léonard, F. Physics of Carbon Nanotube Electronic Devices. *Rep. Prog. Phys.* **2006**, *69*, 507–561.
8. Wang, J. Stripping Analysis at Bismuth Electrodes: A Review. *Electroanalysis* **2005**, *17*, 1341–1346.
9. Baughman, R. H.; Zakhidov, A. A.; De Heer, W. A. Carbon Nanotubes—The Route toward Applications. *Science* **2002**, *297*, 787–792.
10. Liu, Z.; Sun, X.; Nakayama-Ratchford, N.; Dai, H. Supramolecular Chemistry on Water-Soluble Carbon Nanotubes for Drug Loading and Delivery. *ACS nano* **2007**, *1*, 50–56.
11. Jin, L.; Bower, C.; Zhou, O. Alignment of Carbon Nanotubes in a Polymer Matrix by Mechanical Stretching. *Appl. Phys. Lett.* **1998**, *73*, 1197–1199.
12. Andrews, R.; Jacques, D.; Rao, A. M.; Rantell, T.; Derbyshire, F.; Chen, Y.; Chen, J.; Haddon, R. C. Nanotube Composite Carbon Fibers. *Appl. Phys. Lett.* **1999**, *75*, 1329–1331.
13. Shaffer, M. S. P.; Windle, A. H. Fabrication and Characterization of Carbon Nanotube/Poly(vinyl alcohol) Composites. *Adv. Mater.* **1999**, *11*, 937–941.
14. Chen, G. Z.; Shaffer, M. S. P.; Coleby, D.; Dixon, G.; Zhou, W.; Fray, D. J.; Windle, A. H. Carbon Nanotube and Polypyrrole Composites: Coating and Doping. *Adv. Mater.* **2000**, *12*, 522–526.
15. Dai, L.; Mau, A. W. H. Controlled Synthesis and Modification of Carbon Nanotubes and C_{60}: Carbon Nanostructures for Advanced Polymeric Composite Materials. *Adv. Mater.* **2001**, *13*, 899–913.
16. Hirsch, A. Functionalization of Single-Walled Carbon Nanotubes. *Angew. Chem., Int. Ed.* **2002**, *41*, 1853–1859.
17. Sun, Y. P.; Fu, K.; Lin, Y.; Huang, W. Functionalized Carbon Nanotubes: Properties and Applications. *Acc. Chem. Res.* **2002**, *35*, 1096–1104.
18. Huang, W.; Lin, Y.; Taylor, S.; Gaillard, J.; Rao, A. M.; Sun, Y. P. Sonication-Assisted Functionalization and Solubilization of Carbon Nanotubes. *Nano Lett.* **2002**, *2*, 231–234.
19. Kumar, S.; Dang, T. D.; Arnold, F. E.; Bhattacharyya, A. R.; Min, B. G.; Zhang, X.; Vaia, R. A.; Park, C.; Wade Adams, W.; Hauge, R. H.; *et al*. Synthesis, Structure, and Properties of PbO/SWNT Composites. *Macromolecules* **2002**, *35*, 9039–9043.
20. Suslick, K. S. Sonochemistry. *Science* **1990**, *247*, 1439–1445.
21. Suslick, K. S.; Gawlenowski, J. J.; Schubert, P. F.; Wang, H. H. Alkane Sonochemistry. *J. Phys. Chem.* **1983**, *87*, 2299–2301.
22. Zhang, Y.; Shi, Z.; Gu, Z.; Iijima, S. Structure Modification of Single-Wall Carbon Nanotubes. *Carbon* **2000**, *38*, 2055–2059.
23. Monthioux, M.; Smith, B. W.; Burteaux, B.; Claye, A.; Fischer, J. E.; Luzzi, D. E. Sensitivity of Single-Wall Carbon Nanotubes to Chemical Processing: An Electron Microscopy Investigation. *Carbon* **2001**, *39*, 1251–1272.
24. Salzmann, C. G.; Llewellyn, S. A.; Tobias, G.; Ward, M. A. H.; Huh, Y.; Green, M. L. H. The Role of Carboxylated Carbonaceous Fragments in the Functionalization and Spectroscopy of a Single-Walled Carbon-Nanotube Material. *Adv. Mater.* **2007**, *19*, 883–887.
25. Brodie, B. C. Sur Le Poids Atomique Du Graphite. *Ann. Chim. Phys.* **1860**, *59*, 466–472.
26. Staudenmaier, L. Verfahren zur Darstellung der Graphitsäure. *Ber. Dtsch. Chem. Ges.* **1898**, *31*, 1481–1487.
27. Hummers, W. S., Jr; Offeman, R. E. Preparation of Graphitic Oxide. *J. Am. Chem. Soc.* **1958**, *80*, 1339–1339.
28. Park, S.; Ruoff, R. S. Chemical Methods for the Production of Graphenes. *Nat. Nanotechnol.* **2009**, *4*, 217–224.
29. Novoselov, K. S.; Geim, A. K.; Morozov, S. V.; Jiang, D.; Zhang, Y.; Dubonos, S. V.; Grigorieva, I. V.; Firsov, A. A. Electric Field in Atomically Thin Carbon Films. *Science* **2004**, *306*, 666–669.
30. Geim, A. K.; Novoselov, K. S. The Rise of Graphene. *Nat. Mater.* **2007**, *6*, 183–191.
31. Baek, J. B.; Lyons, C. B.; Tan, L. S. Covalent Modification of Vapour-Grown Carbon Nanofibers *via* Direct Friedel-Crafts Acylation in Polyphosphoric Acid. *J. Mater. Chem.* **2004**, *14*, 2052–2056.
32. Choi, J. Y.; Tan, L. S.; Baek, J. B. Self-Controlled Synthesis of Hyperbranched Poly(ether ketone)s from $A_3 + B_2$ Approach *via* Different Solubilities of Monomers in the Reaction Medium. *Macromolecules* **2006**, *39*, 9057–9063.
33. Lee, H. J.; Han, S. W.; Kwon, Y. D.; Tan, L. S.; Baek, J. B. Functionalization of Multiwalled Carbon Nanotubes with Various 4-Substituted Benzoic Acids in Mild Polyphosphoric Acid/Phosphorous Pentoxide. *Carbon* **2008**, *46*, 1850–1859.
34. Fréchet, J. M. J. Functional Polymers and Dendrimers: Reactivity, Molecular Architecture, and Interfacial Energy. *Science* **1994**, *263*, 1710–1715.
35. Paloniemi, H.; Aäritalo, T.; Laiho, T.; Liuke, H.; Kocharova, N.; Haapakka, K.; Terzi, F.; Seeber, R.; Lukkari, J. Water-Soluble Full-Length Single-Wall Carbon Nanotube Polyelectrolytes: Preparation and Characterization. *J. Phys. Chem. B* **2005**, *109*, 8634–8642.
36. Zhao, B.; Hu, H.; Yu, A.; Perea, D.; Haddon, R. C. Synthesis and Characterization of Water Soluble Single-Walled Carbon Nanotube Graft Copolymers. *J. Am. Chem. Soc.* **2005**, *127*, 8197–8203.
37. Shin, Y. R.; Jeon, I. Y.; Baek, J. B. Stability of Multiwalled Carbon Nanotubes in Commonly Used Acidic Media. *Carbon* **2012**, *50*, 1465–1476.
38. Shu, C. F.; Leu, C. M.; Huang, F. Y. Synthesis, Modification, and Characterization of Hyperbranched Poly(Ether Ketones). *Polymer* **1999**, *40*, 6591–6596.
39. Jiang, L.; Gao, L.; Sun, J. Production of Aqueous Colloidal Dispersions of Carbon Nanotubes. *J. Colloid Interface Sci.* **2003**, *260*, 89–94.
40. Li, D.; Müller, M. B.; Gilje, S.; Kaner, R. B.; Wallace, G. G. Processable Aqueous Dispersions of Graphene Nanosheets. *Nat. Nanotechnol.* **2008**, *3*, 101–105.
41. Wellisch, E.; Gipstein, E.; Sweeting, O. J. Thermal Decomposition of Sulfinic Acids. *J. Org. Chem.* **1962**, *27*, 1810–1812.
42. Sorescu, D. C.; Jordan, K. D.; Avouris, P. Theoretical Study of Oxygen Adsorption on Graphite and the (8,0) Single-Walled Carbon Nanotube. *J. Phys. Chem. B* **2001**, *105*, 11227–11232.
43. Bourg, M. C.; Badia, A.; Bruce Lennox, R. Gold-Sulfur Bonding in 2d and 3d Self-Assembled Monolayers: XPS Characterization. *J. Phys. Chem. B* **2000**, *104*, 6562–6567.
44. Krueger, B. J.; Grassian, V. H.; Iedema, M. J.; Cowin, J. P.; Laskin, A. Probing Heterogeneous Chemistry of Individual Atmospheric Particles Using Scanning Electron Microscopy and Energy-Dispersive X-ray Analysis. *Anal. Chem.* **2003**, *75*, 5170–5179.

45. Han, J. T.; Kim, S. Y.; Woo, J. S.; Jeong, H. J.; Oh, W.; Lee, G. W. Hydrosen-Bond-Driven Assembly of Thin Multiwalled Carbon Nanotubes. *J. Phys. Chem. C* **2008**, *112*, 15961–15965.
46. Yu, D.; Nagelli, E.; Du, F.; Dai, L. Metal-Free Carbon Nanomaterials Become More Active Than Metal Catalysts and Last Longer. *J. Phys. Chem. Lett.* **2010**, *1*, 2165–2173.
47. Bard, A. J.; Faulkner, L. R. Fundamentals and Applications. *In Electrochemical Methods*, 2nd ed.; Wiley: New York, 2001.
48. Tammeveski, K.; Tenno, T.; Claret, J.; Ferrater, C. Electrochemical Reduction of Oxygen on Thin-Film Pt Electrodes in 0.1 M KOH. *Electrochim. Acta* **1997**, *42*, 893–897.
49. Lee, J. S.; Kim, S. T.; Cao, R.; Choi, N. S.; Liu, M.; Lee, K. T.; Cho, J. Metal-Air Batteries with High Energy Density: Li-Air *versus* Zn-Air. *Adv. Energy Mater.* **2011**, *1*, 34–50.